Optics Letters

Speckle reduced holographic displays using tomographic synthesis

Seungjae Lee, Dongyeon Kim, Seung-Woo Nam, and Byoungho Lee*

School of Electrical and Computer Engineering, Seoul National University, Gwanak-Gu Gwanakro 1, Seoul 08826, South Korea
**Corresponding author: byoungho@snu.ac.kr*

Received 5 June 2020; revised 19 July 2020; accepted 24 July 2020; posted 24 July 2020 (Doc. ID 399623); published 18 August 2020

Despite significant merit of depth representation, holographic displays have a considerable limitation: speckle. Here, we present speckle reduced holographic displays using an engineered light source with angle diversity for speckle reduction. The level of angle diversity is optimized with consideration of resolution, speckle contrast, and depth of field. To extend the depth of field sacrificed for speckle reduction, we apply tomographic synthesis, exploiting synchronization of a local illumination module and a tunable-focus lens. We implement a benchtop prototype to verify the proposed method, which reduces the speckle contrast averagely by 37.8% while preserving resolution and 4.0 diopter depth of field.

https://doi.org/10.1364/OL.399623

Holographic displays have recently received broad interest, as various researches demonstrate the competence in near-eye displays. Reconstructing an arbitrary wavefront using a spatial light modulator (SLM) for phase or amplitude modulation, holographic displays provide focus cues. Compared to other display approaches (e.g., light field [1] and volumetric displays [2]) to provide focus cues, holographic display prototypes [3,4] have reported superior performance in terms of form factor, field of view, or resolution. However, holographic displays have a significant limitation, speckle, which is induced by a coherent illumination [5]. Generated by a randomized interference (i.e., "random walk") of the coherent illumination, speckle degrades the signal-to-noise-ratio (SNR) of reconstructed images. Furthermore, the speckle phenomenon raises the safety issue of the human visual system because the local intensity can potentially reach a hazardous level.

Despite extensive discussion [5] for speckle reduction methods in a coherent optical system, it is challenging to adopt those methods for holographic displays. Most speckle reduction methods superimpose independent speckle patterns generated by increasing angle or wavelength diversity of a light source [6–8]. Lee *et al*. [8] introduced a method to increase the angle diversity by an optical superposition. However, the increase in diversity involves a sacrifice of resolution or depth of field (DoF) in holographic displays [9]. An alternative method for speckle reduction is to refresh holograms on the SLM at a fast frame rate for temporal superposition of independent speckle patterns [10–12]. Although it is the only method for speckle reduction without the trade-off of resolution, the sacrifice of frame rate or bit depth is a significant bottleneck of this approach.

Here, we aim to reduce the speckle contrast of holographic displays while maintaining resolution, DoF, and frame rate. In other words, our goal is to extend the limited DoF of speckle reduced holographic displays. To compensate for the DoF sacrifice, we apply a tomographic synthesis method [2] that enables a 2D display to reconstruct a volumetric scene. In this Letter, a speckle reduced holographic display substitutes for the 2D display. The limited DoF of the speckle reduced holographic display is compensated for by the tomographic synthesis, while the holographic reconstruction contributes to the accurate and dense depth representation. A schematic diagram of the intuitive exposition of the proposed approach is illustrated in Fig. 1. We employ a tunable-focus lens (TFL) and a local illumination module (LIM). The LIM divides the SLM into multiple sub-SLMs that reconstruct the corresponding sub-holograms. As illustrated in Figs. 1(b) and 1(c), we adjust the target scene's depth to reconstruct sub-holograms mostly within a DoF of speckle reduced holographic display. The TFL compensates for the depth adjustment, and the observer eventually perceives accurate depth cues. The synchronization of the TFL and the LIM allows the TFL to have the desired focal power for each sub-hologram. If a round trip of the change in the TFL's focal length is finished in less than 1/60 s, sub-holograms are temporally fused to reconstruct the volumetric target scene.

To verify the proposed concept, we implement a prototype with the fundamental structure of holographic displays shown in Fig. 1. The prototype consists of an LIM (532 nm), a collimating lens, an SLM (3.74 μm pixel pitch, 3840 × 2160), a TFL (EL-10-30-TC-VIS-12D, Optotune) separated by 125 mm from the SLM, and an observation system. We assume that the observer wears the TFL and the eye-relief distance between the TFL and the eye-lens is negligible. The detailed specifications of elements are determined to satisfy the target display performance while minimizing the speckle contrast. Considering the human visual system of normal vision, the target performance includes the exit-pupil (10 mm), resolution (30 cycles per degree, cpd) [13], and DoF (25 cm to optical 90 infinity) [14]. The exit-pupil size of the system w_p is given by $\lambda z_u/p$, where p is the pixel pitch of the SLM. As the pixel pitch is 3.74 μm and the wavelength is 532 nm, the distance of z_u is given by 70 mm for the 10 mm exit-pupil.

0146-9592/20/174686-04 Journal © 2020 Optical Society of America

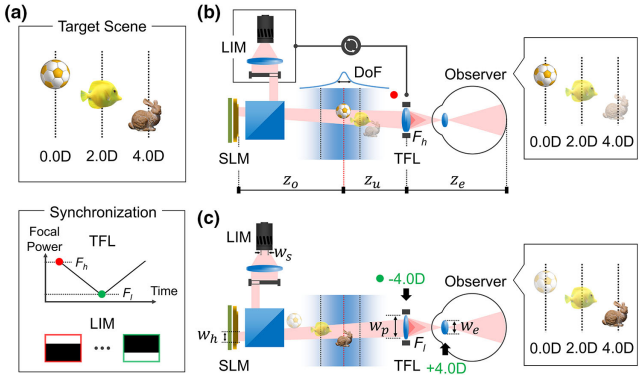

Fig. 1. Schematic diagram to illustrate the principle of speckle reduced holographic displays using tomographic synthesis. (a) We aim to reconstruct a target scene of 4.0 diopter (D) depth range with the synchronization of a LIM and a TFL. When the focal power of the TFL is (b) F_h or (c) F_l, corresponding sub-SLM is locally illuminated for the reconstruction of a ball or a bunny. Note that the depth adjustment of the target scene is compensated for by the focal power modulation of the TFL.

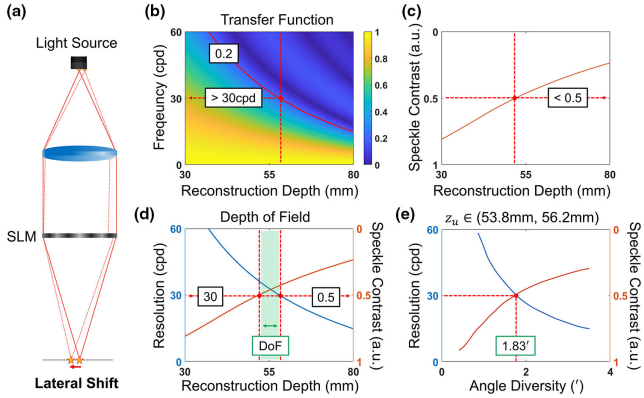

Fig. 2. (a) Lateral shift of holographic reconstruction by angle diversity. (b) Transfer function and (c) speckle contrast according to the reconstruction depth. In this simulation, we suppose an engineered light source with the angle diversity of $\pm 0.92'$ ($1.83'$ in total). (d) Criterion to estimate the DoF in speckle reduced holographic displays. The DoF is determined by a region where the resolution is higher than 30 cpd, and the speckle contrast is less than 0.5. (e) Lower and upper bounds of the resolution and the speckle contrast within the reconstruction depth range of (53.8 mm, 56.2 mm) according to the angle diversity. Exploiting this result, we can select a light source that minimizes the speckle contrast while maintaining 30 cpd resolution.

Compared to the exit-pupil, achievement of the target resolution or DoF is more complicated because it requires understanding the effects of angle diversity of the light source on holographic displays. The angle diversity of the light source leads to the lateral shift of reconstructed holograms [5,9], as illustrated in Fig. 2(a). If the spatial coherence of the light source is limited, the laterally shifted holograms are incoherently integrated. The hologram integration is interpreted by the convolution of the lateral shift function and the original hologram. The convolution corresponds to the multiplication in the Fourier domain, which is given by

$$I_s(\mathbf{v}) = A(\mathbf{v})\, I_o(\mathbf{v}), \tag{1}$$

where I_s, $A(\mathbf{v})$, and I_o are Fourier transforms of the laterally integrated hologram, the shift function, and the original hologram, respectively. $\mathbf{v}$ is the spatial frequency represented by (v_x, v_y), referred to as x and y components. When the light source has an angle diversity of θ_s, Fourier transform of the observed image, I_g, is given by

$$\begin{aligned} I_g(M\mathbf{v}) &= T(\mathbf{v})\mathrm{sinc}\,(\theta_s z_o v_x)\ \mathrm{sinc}\left(\theta_s z_o v_y\right) I_o(\mathbf{v}) \\ &= T_p(\mathbf{v})\, I_o(\mathbf{v}), \end{aligned} \tag{2}$$

where $T(\mathbf{v})$ is the transfer function of the imaging system [15] that has a magnification factor of M. Finally, we can derive the transfer function abs(T_p) of speckle reduced holographic displays. Using this equation, we establish the transfer function map in Fig. 2(b) to evaluate the resolution of holographic displays. In this figure, a red contour represents the resolution limit frequency for which the transfer function reduced to 0.2.

As shown in Eq. (2), the resolution is related to the light source angle diversity θ_s and the reconstruction depth z_o. These variables are also related to the speckle contrast of the observed image. In holographic displays exploiting the angle diversity, the speckle decorrelation by a lateral shift is a dominant term to determine the level of speckle reduction. In the observation plane, the lateral shift range of the speckle pattern is given by

$$\Delta x \in \left(-\frac{w_s}{2z_s} M z_o,\ \frac{w_s}{2z_s} M z_o\right), \tag{3}$$

where Δx is the lateral shift [16]. The speckle decorrelation condition by the lateral shift is determined by the speckle size. In the imaging system, the speckle size is given by $\lambda z_e / w_e$. λ is the light source wavelength, z_e is the distance between the imaging lens and the sensor, and w_e is the pupil width [5]. Thus, the number of independent speckle patterns generated by the light source is given by

$$n_a = \left(1 + \frac{w_s w_e z_o}{\lambda z_s z_u}\right)^2, \tag{4}$$

where n_a is the number of independent speckles, and z_u is the distance between the imaging lens and the reconstructed hologram. Note that the number of independent speckle patterns is raised to the power of two because the angle diversity has two axes. Using this equation, we plot the speckle contrast, given by $1/\sqrt{n_a}$, in Fig. 2(c).

As described in Eqs. (2) and (4), the resolution and the speckle contrast have correlation with the angle diversity θ_s and the hologram reconstruction depth z_o. It is noticeable that both the resolution and the speckle contrast are related to the reconstruction depth, as demonstrated in Figs. 2(b) and 2(c). Using this relationship, we can define a depth range where specific requisites for the resolution and the speckle contrast are satisfied. For example, we suppose a region where the resolution is higher than 30 cpd, and the speckle contrast is less than 0.5. The depth range of this region could be a criterion to determine the DoF in speckle reduced holographic displays, as shown in Fig. 2(d). Exploiting the criterion, we can optimize the angle diversity to minimize the speckle contrast while attaining 30 cpd resolution and a specific DoF. If the DoF requirement of each sub-hologram is 0.5 diopter (D), the corresponding depth range would be (53.8 mm, 56.2 mm). Figure 2(e) shows the lower and

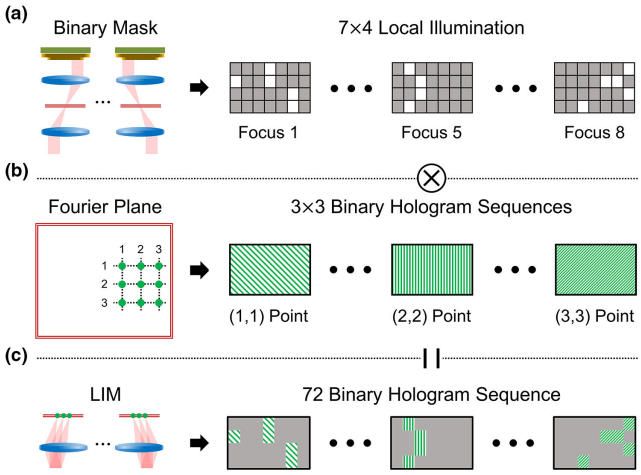

Fig. 3. Block diagram to describe the DMD operation in our prototype. (a) The DMD's first role is an active binary mask for local illumination using eight frames, and (b) the second role is to increase the angle diversity of the light source using nine frames. (c) In total, a 72 binary hologram sequence is generated by the convolution of the two binary sequences.

upper bounds of the resolution and the speckle contrast within this depth range. As shown in this figure, the angle diversity of $\pm 0.92'$ guarantees the maximum speckle reduction by 0.47 while securing the 30 cpd resolution.

Gathering all determined or optimized variables, we determine the requirements of the LIM in the proposed system. To extend the limited DoF (0.5 D) to 4.0 D (25 cm to optical infinity), the required depth resolution of tomographic synthesis is eight. The spatial resolution of the LIM, the number of sub-SLMs, is set as 7×4 with consideration of the 30 cpd diffraction limit and the vignetting effect. Accordingly, the desired specifications of the LIM are eight depth resolution at 60 Hz and 7×4 spatial resolution. To implement the LIM with the above specifications, we use a digital micromirror device (DMD, 10.8 μm pixel pitch, 1920×1080, 23148 Hz). In our prototype, the DMD has two roles: local illumination of the SLM shown in Fig. 3(a) and increasing angle diversity of the coherent illumination shown in Fig. 3(b). As illustrated in Fig. 3(a), the DMD panel is relayed to the SLM plane so that the DMD panel performs the role of an active binary mask. Note that the active binary mask is refreshed eight times within 1/60 s for eight depth resolution of tomographic synthesis.

Second, the DMD increases the angle diversity of the coherent light source (laser diode, 532 nm) via temporal multiplexing. The DMD displays a sequence of binary sub-holograms (270×270) that reconstruct point sources at the Fourier plane of the relay system. The temporal multiplexing of multiple binary holograms imitates an array of independent point sources (532 nm), which corresponds to an engineered light source. The point sources are distributed to appropriate positions for the optimal angle diversity of the engineered light source. The DMD allocates nine frames for temporal multiplexing of the binary holograms, resulting in 3×3 point sources. In total, 4320 Hz refresh rate of the DMD (72 frames within 1/60 s) is necessary to support the local illumination and increase the angle diversity. Figure 3 illustrates a block diagram that describes the procedure to generate a 72 binary hologram

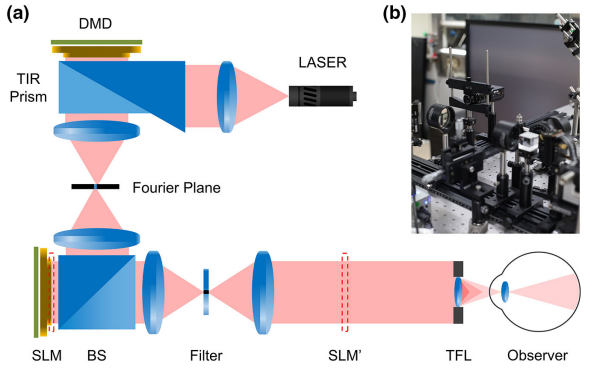

Fig. 4. Demonstration of the benchtop prototype. We present (a) a schematic diagram and (b) a photograph.

sequence. Note that there could be other candidates for the LIM, including an LED array, a bundle of optical fibers [5], and microelectromechanical system scanning backlight with a random diffuser.

Figure 4 demonstrates the implemented benchtop prototype. For the relay optics of the DMD, we use a pair of lenses of 150 mm focal length. Binary holograms for the point source reconstruction are generated by following a precedent research [17]. Each point source is reconstructed at the Fourier plane and collimated by the second lens. We place a Fourier filter (500 μm pinhole) to remove undesired signals from binary holograms (e.g., surface reflection, high order, and ambiguity). The phase-only SLM modulates the local illumination, and the corresponding sub-hologram is reconstructed. Each sub-hologram is obtained by cropping a full-size hologram generated by a layer-based algorithm [18]. The full-size hologram is calculated after the corresponding depth adjustment illustrated in Fig. 1. Additional 4F relay optics (a pair of lenses of 75 mm focal length) removes the zero/high-order noises. Finally, the reconstructed sub-holograms are floated by the TFL that periodically modulates the focal power (10.28 D to 14.28 D) at 60 Hz. The TFL and the LIM are synchronized for temporal multiplexing of the sub-holograms. Note that the tomographic synthesis involves 1.6% average loss of the exit-pupil.

In the experiment, we design an observation system that imitates the human visual system. The observation system consists of a c-mount lens (F/6D, 25 mm focal length), and a charge-coupled device (CCD) (GS3-U3-91S6C-C, FLIR). The c-mount lens and the CCD correspond to the eye-lens and the retina. In this configuration, the mean value of z_e is 26.4 mm, and the pupil width is 2 mm. The pupil width is estimated by the speckle size measured as 6.65 μm. Figure 5 demonstrates experimental results captured by the observation system for comparison of conventional and proposed holographic displays. We digitally combined RGB color channel images to investigate how speckles would be observed in a full-color system. As demonstrated in the results, the tomographic synthesis using the TFL allows the reliable display performance within 4.0 D DoF. The prototype reduces the speckle contrast to 0.31 from 0.82 while preserving the resolution and the 4.0 D DoF. The speckle reduction level corresponds to 37.8% (~7 independent speckle integration) in the experiment. The observed speckle reduction is more significant than the theoretical prediction of 47% (~5 independent speckle integration). We believe this difference is involved with the tomographic synthesis, where the TFL

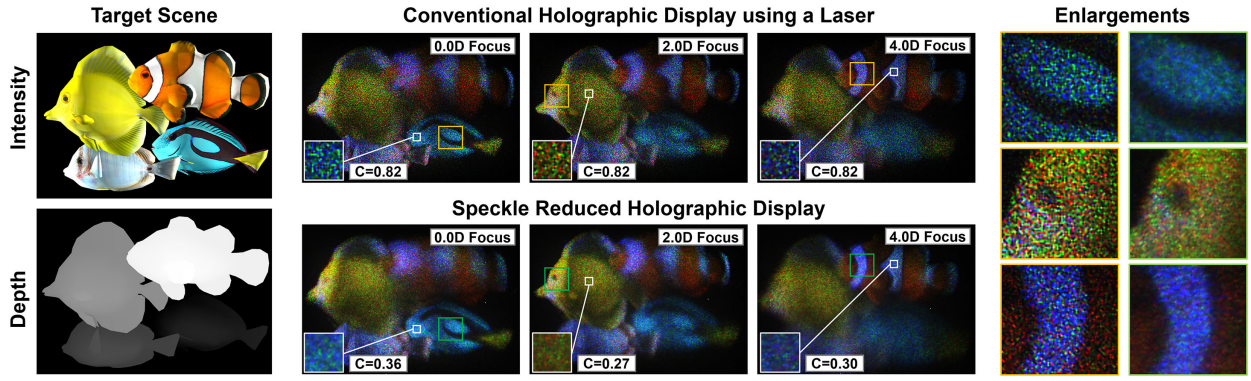

Fig. 5. Experimental results to compare conventional and speckle reduced holographic displays. Speckle reduced holographic displays reduce the speckle contrast averagely by 37.8%. The speckle contrast (C) is extracted from a cropped image (30 × 30 pixels). We also confirm that the resolution reduction is minimized within the 4.0 D DoF. The intensity and depth information of a volumetric target scene is presented in the leftmost figures. Note that RGB color images are presented to give an intuition of how speckle would be observed in practical use. We digitally combine each color channel image captured with a single wavelength (532 nm).

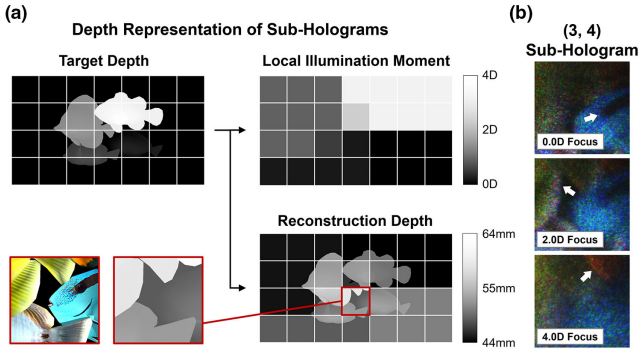

Fig. 6. (a) Depth conversion process to determine local illumination moment and generate sub-holograms. (b) Although the LIM has limited resolution and refresh rate, depth representation of sub-hologram is dense and accurate.

continuously modulates the focal power. Each sub-hologram could be reconstructed with some optical blur, which further reduces the speckle contrast.

The proposed method also has the merit of volumetric reconstruction of sub-holograms. As illustrated in Fig. 6(a), the spatial and depth resolutions of the LIM are limited to 7 × 4 and 8, respectively. Nevertheless, the sub-hologram reconstruction ensures the depth representation to be accurate, as shown in Fig. 6(b). The sub-hologram reconstruction is a significant advantage compared to conventional tomographic displays using a low-resolution or low-frame-rate backlight module [2]. Without holographic reconstruction, each sub-SLM display depth is fixed to a constant depth. Accordingly, combining holographic and tomographic display methodologies relaxes the LIM requisite of the spatial resolution and the refresh rate.

In conclusion, we introduced the speckle reduced holographic display using tomographic synthesis. The proposed method intentionally increased the angle diversity of the coherent illumination to 1.83′ for speckle reduction. The angle diversity level was optimized to minimize the speckle contrast while securing 30 cpd resolution and 0.5 D DoF. The 0.5 D limited DoF was extended to 4.0 D by tomographic synthesis, which exploits synchronization of the LIM and the TFL. We implemented and demonstrated the prototype with a comparison between the conventional and proposed methods. The experimental results showed that our approach could reduce the speckle contrast averagely by 37.8% while the resolution and the 4.0 D DoF were preserved. Leveraging the advantages of holographic and tomographic display technologies, we mitigated the drawback of speckle reduction in holographic displays.

Funding. Institute for Information and Communications Technology Promotion under Government of Korea (MSIT) (2017-0-00787).

Disclosures. The authors declare no conflicts of interest.

REFERENCES

1. N. Matsuda, A. Fix, and D. Lanman, ACM Trans. Graph. **36**, 86 (2017).
2. S. Lee, Y. Jo, D. Yoo, J. Cho, D. Lee, and B. Lee, Nat. Commun. **10**, 2497 (2019).
3. A. Maimone, A. Georgiou, and J. S. Kollin, ACM Trans. Graph. **36**, 85 (2017).
4. C. Jang, K. Bang, G. Li, and B. Lee, ACM Trans. Graph. **37**, 195 (2018).
5. J. W. Goodman, *Speckle Phenomena in Optics: Theory and Applications*, 2nd ed. (SPIE, 2020).
6. E. Moon, M. Kim, J. Roh, H. Kim, and J. Hahn, Opt. Express **22**, 6526 (2014).
7. T. Kozacki and M. Chlipala, Opt. Express **24**, 2189 (2016).
8. D. Lee, C. Jang, K. Bang, S. Moon, G. Li, and B. Lee, IEEE Trans. Ind. Inf. **15**, 6170 (2019).
9. Y. Deng and D. Chu, Sci. Rep. **7**, 5893 (2017).
10. Y. Takaki and M. Yokouchi, Opt. Express **19**, 7567 (2011).
11. Y. Mori, T. Fukuoka, and T. Nomura, Appl. Opt. **53**, 8182 (2014).
12. B. Lee, D. Yoo, J. Jeong, S. Lee, D. Lee, and B. Lee, Opt. Lett. **45**, 2148 (2020).
13. A. Patney, M. Salvi, J. Kim, A. Kaplanyan, C. Wyman, N. Benty, D. Luebke, and A. Lefohn, ACM Trans. Graph. **35**, 179 (2016).
14. V. F. Pamplona, A. Mohan, M. M. Oliveira, and R. Raskar, ACM Trans. Graph. **29**, 77 (2010).
15. J. W. Goodman, *Introduction to Fourier Optics*, 4th ed. (W.H. Freeman, 2017).
16. I. Yamaguchi, Opt. Acta **28**, 1359 (1981).
17. W.-H. Lee, Appl. Opt. **18**, 3661 (1979).
18. H. Zhang, L. Cao, and G. Jin, Appl. Opt. **56**, F138 (2017).